Published in final edited form as:
Hear Res. 2013 October ; 304: 159–166. doi:10.1016/j.heares.2013.07.013.

Gentamicin administration on the stapes footplate causes greater hearing loss and vestibulotoxicity than round window administration in guinea pigs

E.B. King[1,2], **A.N. Salt**[3], **G.E. Kel**[1], **H.T. Eastwood**[1], and **S.J. O'Leary**[1]

[1]Department of Otolaryngology, University of Melbourne, Melbourne, VIC Australia

[2]Bionics Institute, Melbourne VIC Australia

[3]Department of Otolaryngology, Washington University School of Medicine, St Louis, MO, USA

Abstract

Clinically, gentamicin has been used extensively to treat the debilitating symptoms of Mèniére's disease and is well known for its vestibulotoxic properties. Until recently, it was widely accepted that the round window membrane (RWM) was the primary entry route into the inner ear following intratympanic drug administration. In the current study, gentamicin was delivered to either the RWM or the stapes footplate of guinea pigs (GPs) to assess the associated hearing loss and histopathology associated with each procedure. Vestibulotoxicity of the utricular macula, saccular macula, and crista ampullaris in the posterior semicircular canal were assessed quantitatively with density counts of hair cells, supporting cells, and stereocilia in histological sections. Cochleotoxicity was assessed quantitatively by changes in threshold of auditory brainstem responses (ABR), along with hair cell and spiral ganglion cell counts in the basal and second turns of the cochlea. Animals receiving gentamicin applied to the stapes footplate exhibited markedly higher levels of hearing loss between 8–32kHz, a greater reduction of outer hair cells in the basal turn of the cochlea and fewer normal type I cells in the utricle in the vestibule than those receiving gentamicin on the RWM or saline controls. This suggests that gentamicin more readily enters the ear when applied to the stapes footplate compared with RWM application. These data provide a potential explanation for why gentamicin preferentially ablates vestibular function while preserving hearing following transtympanic administration in humans.

Keywords

Inner ear drug delivery; gentamicin; pharmacokinetics; oval window; stapes; stapediovestibular joint; annular ligament

1. Introduction

Local drug delivery has distinct advantages for the treatment of inner ear disease, including targeted therapy and elimination of the risk of systemic drug-related side effects. This

Author Contact Information: Elisha King, Bionics Institute, 384-388 Albert Street, East Melbourne VIC 3002, Australia. Telephone: +61 3 9288 2989, Eking@bionicsinstitute.org.

approach has a place in the clinical treatment of Mèniére's Disease and sudden sensorineural hearing loss. It has been widely accepted that drugs delivered to the middle ear space during local delivery primarily enter the inner ear via permeation through the round window membrane (RWM) into scala tympani (ST), with subsequent diffusion into scala vestibuli (SV) and the vestibule through the interstitial spaces of the spiral ligament (Salt & Ma, 2001; Salt et al., 2003; Plontke et al., 2007) and into Rosenthal's canal via caniculi perforantes (Shepherd & Colreavy, 2004). Trans-osseous drug entry has also been reported to occur through the bone of the otic capsule in rodent models (Mikulec et al., 2009). Qualitative data from some investigators has suggested that substances could enter vestibular perilymph through the oval window (OW) (Tanaka & Motomura, 1981; Saijo & Kimura, 1984; Zou et al., 2005). We have previously reported results consistent with this. In a Magnetic Resonance Imaging (MRI) study (King et al., 2011), significantly higher Gadolinium (Gd) based contrast agent was observed in the vestibule and SV than expected from round window entry, following intratympanic delivery in the guinea pig model. The amount of Gd in SV and the vestibule could not be explained by entry through the RWM alone. Rather, it was calculated that up to 90% of the Gd had entered the vestibule directly in the vicinity of the stapes footplate. It is evident in other MRI studies in rats and humans that Gd signal is higher in the vestibule than in ST. This is consistent with the interpretation that the Gd marker may have entered the inner ear via the annular ligament of the stapediovestibular joint (SVJ) (Zou et al., 2005; Zou et al., 2012).

Direct drug entry into the vestibule in the vicinity of the stapes footplate was subsequently confirmed using ionic marker trimethylphenlyammonium (TMPA) following intracochlear injections or applications to the round window (RW) niche, with or without occlusion of the RW membrane or stapes area (Salt et al., 2012). In that study, perilymph TMPA concentrations were monitored either in real time with TMPA-selective microelectrodes sealed into ST and SV, or by the collection of sequential samples of perilymph from the lateral semi-circular canal. When the RWM was occluded, round window niche irrigation produced higher concentrations in SV compared to ST, confirming direct TMPA entry into the vestibule in the region of the stapes. Additionally, the TMPA levels of initial samples (originating from the vestibule) were markedly lower when the stapes area was occluded. This demonstrated that entry through the oval window greatly influences the level of drug in vestibular perilymph. As a result, the concentration of drugs in the vestibule may be considerably higher following intratympanic administration than previously recognized based on entry through the RWM alone.

Clinically, aminoglycoside antibiotic gentamicin may be administered intratympanically to relieve the debilitating symptoms of vertigo associated with Mèniére's disease (Lange, 1977; Silverstein et al., 1999). The symptoms of Mèniére's disease largely result from fluctuations of vestibular and auditory function associated with endolymphatic hydrops. In severe cases of Mèniére's disease, one approach has been to control vertigo attacks by suppressing vestibular function with gentamicin. Gentamicin is toxic to the cochlea and vestibular organs, affecting both hearing and balance (Govaerts et al., 1990). In the vestibular neuroepithelium, type I hair cells are known to be most susceptible to gentamicin as these cells more avidly take up or retain the drug in the early period after administration (Lopez et al., 1997; Lyford-Pike et al., 2007; Hirvonen et al., 2005; Tanyeri et al., 1995). Ototoxicity is an undesirable potential side effect of intratympanic gentamicin therapy, and the risk of hearing loss increases proportionately with gentamicin dosage (concentration, volume and administration time) (Plontke et al., 2002; Salt et al., 2008). Attempts to deliver gentamicin more specifically to the vestibule, by surgically occluding the RWM with connective tissue before intratympanic injection of a high drug concentration, did not markedly affect patient outcome; specifically a significant number of patients (27%) still experienced hearing loss (Quaranta et al., 1999).

In light of these considerations and the findings from our previous studies, it is of clinical interest to understand whether gentamicin enters the inner ear via the oval window. If so, then there is a possibility that with optimization of the delivery technique, it may be possible to target the vestibule directly with gentamicin thereby potentially minimizing the risk of ototoxicity during aminoglycoside therapy for Mèniére's disease. Here we explore functional and morphological effects of aminoglycoside toxicity upon the cochlea and vestibular systems when gentamicin is targeted to either the OW or to the RWM. Hearing thresholds and histological damage to cells in the cochlea and vestibule were compared after a highly concentrated gentamicin solution was delivered directly onto the RWM or OW. Saline control groups for each treatment group were used to control for the effects of the surgery.

2. Materials and Methods

2.1. Animal Preparation

The study was approved by the Royal Victorian Eye and Ear Hospital (Melbourne, Australia) Animal Ethics Committee (Ethics Approval 11/238AR). Twenty-two tri-colour adult guinea pigs (Dunkin-Hartley strain) of either sex, weighing between 397–851g, were used in the study and randomly assigned to a treatment group. The age of the animals in both gentamicin treatment groups were similar. The animals were anaesthetized with ketamine (Troy Laboratories Pty Ltd, Australia; 60 mg/kg) and xylazil-20 (Troy Laboratories Pty Ltd, Australia; 4 mg/kg) administered intramuscularly. Anesthesia was monitored during the experiment using pedal and ocular reflexes and supplemented as necessary with 67% of the initial dose. 0.5–1 ml of Lignocaine-20 (Troy Laboratories Pty Ltd, Australia) was administered subcutaneously to the surgical site prior to making the incision. Temgesic (0.05 mg/kg) and Endotril (Troy Laboratories Pty Ltd, Australia; 20 mg/kg) were administered sub-cutaneously following surgery for analgesia and infection control respectively.

2.2. Materials

Three microliters of a 337 mg/ml solution (1 mg total) of gentamicin sulfate (G3632-5g, Sigma Aldrich) in phosphate buffered saline was administered either onto the stapes footplate or onto the RWM. The solution was delivered with a 5 μL Hamilton syringe fitted with a with 32 gauge flat tip needle (SGE Analytical Science Pty Ltd, Australia) connected to a syringe driver (Micro4™Microsyringe Pump, World Precision Instruments, USA). For the control cohorts, 3 μL of 0.9% normal saline (Promed, Thermofisher Scientific) was administered onto the stapes footplate or onto the RWM.

2.3. Surgical Procedure

Using a dorsolateral posterior-auricular surgical approach, the bulla of one ear was opened using a 1.5 mm diameter cutting burr under the operating microscope to expose the round window and stapes footplate. The treatment solution was administered directly on to the footplate of the stapes (gentamicin n=5, saline n=4) or RWM (gentamicin n=4, saline n=4). Following delivery, the animal was left in position for 30 minutes to allow the drug to permeate the structure. Any visible excess fluid was wicked away with a paper tissue wick, the wound was sutured closed. At one week after treatment, animals were anesthetized for auditory brainstem response recording and then euthanized with an intraperitoneal injection of 0.5mg/kg Lethabarb (Virbac Pty Ltd, Australia). The inner ears were removed for histological analysis.

2.4. Auditory brainstem response recordings

Acoustically evoked auditory brainstem responses (ABR) were measured prior to the first surgery and a final ABR was performed one week after treatment to measure auditory function in the treated ear. The change in ABR threshold was calculated as the difference between the two measurements. ABR recordings were made in a sound-proof Faraday cage whilst the contralateral ear was occluded with an ear mould compound (Otoform, Dreve Germany) to attenuate hearing. Computer generated acoustic stimuli (5 ms tone pips with 1 ms rise/fall times at frequencies 2, 8, 16, 24 and 32 kHz) were delivered free-field from a loudspeaker (Richard Allen DT-20, UK) placed 0.1 m from the ipsilateral pinna. Stimulus intensity was attenuated in 5 dB steps. Brainstem responses were recorded differentially (DAM-5A Differential Preamp, WP Instruments Inc) from subcutaneous needle electrodes placed at the vertex and the nape of the neck. A grounding electrode was placed further caudally in the thigh. The signals were amplified 100,000 times, filtered between 150–3000 Hz, and digitally sampled at 20 kHz. ABR data was analyzed using Igor Pro V6.2 and tabulated in Microsoft Excel V14.1.0.

2.5. Histology

The animal was perfused by an intracardiac injection of heparinsed isotonic saline followed by 10% neutral buffered formalin solution (3.7% Formaldehyde, Fronine Laboratory Supplies, Australia). Both inner ears were removed, fixed in formalin solution for up to 2 weeks, and decalcified in 10% (w/v) ethylenediaminetetraacetic acid (Applichem, Thermofisher Scientific, Australia) for up to 4 weeks. Cochleae were trimmed, aligned in agar and embedded in paraffin wax. Sections of 5 mm thickness were taken every 50 mm, mounted on a glass slide, stained with Hematoxylin (APS Chemicals) and Putt's Eosin (ProSciTech) and cover slipped. The slides were scanned using a x20 objective (Zeiss Mirax digital slide scanner) and analysed with Mirax Viewer software (V 1.12.22.0 Carl Zeiss MicroImaging GmbH, 3D Histech).

2.6. Cochlear histopathology

Inner hair cells (IHCs), outer hair cells (OHCs), and spiral ganglion cells in the lower and upper regions of the basal and second turns were manually counted. IHC and OHC were identified by the presence of a cell nucleus and were counted by three investigators in three consecutive mid-modiolar sections, each separated by 50 mm. The cell counts were averaged across sections. Spiral ganglion cells were counted from a mid-modiolar section in the basal and second turns. Cells were identified by the presence of the nucleus, and densities were calculated by dividing counts by the area of Rosenthal's canal, as measured with Mirax Viewer software (data not shown).

2.7. Vestibular histopathology

Morphological criteria were used to identify and quantify vestibular hair cells and supporting cells (Merchant, 1999; Tanyeri et al., 1995; Lopez et al., 1997; Tsuji et al., 2000; Hirvonen et al., 2005; Desai et al., 2005). Normal type I hair cells (HCs) had flask-shaped cell bodies surrounded by an afferent nerve calyx, a spherical nucleus with heterogeneous chromatin, a stereocilia bundle, and a cuticular plate. Type II HCs were identified by their cylindrical shape, an ovoid nucleus with homogenous chromatin, superficial spatial location in the sensory epithelium, stereocilia bundle and cuticular plate, and the absence of a nerve calyx surrounding the cell body. Supporting cells were characterized by a lightly stained nucleus with chromatin material distributed in clumps, spatially located in an irregular row of monolayer cells adjacent to the basal lamina in the lower third of the sensory epithelium, and these cells lacked stereocilia or a cuticular plate (Lindeman 1969; Lopez et al. 1997; Merchant 1999; Merchant et al. 2010; Tanyeri et al. 1995).

Using the morphology criteria above, cells in the mid-section of utriculi macula, saccular macula, and the crista ampullaris in the posterior semi-circular canal were manually counted. In the case when a nerve calyx contained multiple HCs, each nucleus was counted as a HC, whereas no HC was recorded in the case of calyceal lucency (no nuclei). Abnormal type I hair cells with swollen nerve calyxes, shrunken and distorted nuclei with increased electron density of cytoplasm with thin, spindly or absent afferent nerve branches were not included in the counts. To account for inter-animal variation, the cell counts were normalized to the counts from the respective untreated contralateral structure. To eliminate observer bias, all sections were assessed in a blinded manner using consistent morphological criteria. To calculate the density of hair cells per unit area, the areas of the respective cellular regions were hand-selected and measured in Mirax Viewer, and the HC count was divided by the area.

2.8. Statistical Analysis

Cell counts were subjected to one-way and two-way ANOVA analysis with treatment group and region as factors. Effect sizes were evaluated post hoc using the Holm-Sidak test and pairwise multiple comparisons were evaluated using Student-Newman-Keuls method. When homogeneity as tested by the Shapiro-Wilk method failed, Kruskal-Wallis ANOVA on ranks was performed. Statistical calculations were performed using Sigmaplot V 12.0 (Systat Software Inc.).

3. Results

3.1. Auditory Brainstem Response

Gentamicin, when applied to the stapes (n=5) resulted in higher ABR thresholds across frequencies 2–32 kHz compared to any other group (shown in Figure 1). This was statistically significant when compared to the saline-stapes group (n=4) at frequencies between 8–32kHz (8kHz: $F_{1,8}$=23.183, p<0.005; 16 kHz: H =6.050, df 1, p<0.05; 24 kHz: $F_{1,8}$=6.369, p<0.05; 32 kHz: $F_{1,8}$=10.100, p<0.05, ANOVA). There was a statistically significant difference in ABR thresholds at frequencies 8 & 16 kHz when gentamicin was applied to the stapes compared to the RWM (8 kHz: $F_{1,8}$=7.457, p<0.05; 16 kHz: H=6.102, df 1, p<0.05, ANOVA). In contrast, when gentamicin was applied to the RWM, the elevation of ABR thresholds did not differ significantly at any frequency compared to RWM saline controls (2kHz: $F_{1,7}$=0.000, p>0.05; 8kHz: $F_{1,7}$=0.360, p>0.05; 16 kHz: $F_{1,7}$=1.800, p>0.05; 24 kHz: $F_{1,7}$=0.200, p>0.05; 32 kHz: $F_{1,7}$=0.021, p>0.05, ANOVA).

3.3. Cochlear Morphology

OHC counts in the basal and second turns were lower in the groups receiving gentamicin than their respective saline controls (Figure 2 lower panel). OHC loss was statistically significant in the lower basal (LB) turn in the gentamicin-stapes group compared to saline-stapes controls (H =4.446, df 1, p<0.05, ANOVA) but did not reach statistical significance in any other cochlear region. The differences in OHC counts in the gentamicin-RWM group compared to saline-RWM controls did not reach significance in any region. There were no significant losses of IHCs (Figure 2 upper panel) or spiral ganglion cells (data not shown) in any turn in either of the gentamicin treatment groups compared to their respective saline controls. Figure 3 shows examples of average OHC and IHC morphology in the lower basal turn in Haematoxylin and Eosin stained sections following gentamicin delivered to the stapes footplate (Figure 3A) or RWM (Figure 3B), and their respective saline controls (Figure 3C and 3D).

3.2. Vestibular Morphology

Type I & II hair cells, supporting cells, and stereocilia were manually counted in the striolar and peripheral regions of the saccular macula, utricular macula, and crista ampullaris of the posterior semi-circular canal (PSCC) (shown in Figure 4A). Examples of normal type I & II hair cells and supporting cells are shown in Figure 4B.

The density of type I HCs with normal morphology in each treatment group across the vestibular regions of interest are shown in Figure 5, normalized to the estimates made in the same region of the contralateral ear. The lowest percentage of normal type I HCs occurred in the group receiving gentamicin on the stapes. The decrease was statistically significant in the utricular macula when compared to the saline controls ($F_{1,7}$=9.142, p<0.05, one-way ANOVA). For all structures combined, type I HC counts following gentamicin application on the stapes footplate were significantly lower than saline-stapes, gentamicin-RWM, and saline-RWM ($F_{3,46}$=8.708, p<0.001, two-way ANOVA). The percentage of normal type I cells in the group receiving gentamicin on the RWM was lower than saline-RWM controls but this did not reach statistical significance in any vestibular region (utricle: $F_{1,7}$=1.402, p>0.05; saccule: H=1.125, df 1, p>0.05; crista ampullaris: $F_{1,6}$=0.940, p>0.05, ANOVA). Stereocilia, type II HCs, and supporting cell counts were measured but there were no statistically significant changes observed in any of the regions analysed (data not shown).

Fig. 6 shows average cellular morphology of the crista ampullaris in the posterior semi-circular canal from each treatment group. Extensive damage to type I & II hair cells was observed following gentamicin administration to the stapes footplate (Figure 6 Ai-ii). This was evident by the occurrence of distorted hair cell morphology, swollen nerve calyxes, an increased incidence of calyceal lucency (absence of nuclei), reduced bundles of stereocilia, darker appearance of nuclei, and a narrowing of the cellular layer between the cuticular plate and basal lamina when compared to untreated contralateral ears. In one animal, there were no type I HC nerve calyxes remaining in any region of the treated ear (data not shown). These features are indicative of gentamicin vestibulotoxicity (Lopez et al. 1997; Tanyeri et al. 1995; Nakagawa et al., 1997). A reduction in dark cells was observed in some ears. Following gentamicin delivery on the RWM (Figure 6 Bi-ii), there were fewer normal type I HCs and some cellular abnormality compared to untreated contralateral ears, however the majority of cells exhibited normal morphological appearance. Figure 6 Ci-ii and Di-ii show cellular morphology following saline administered to the stapes footplate or RWM respectively. Cells in these groups exhibited normal morphology.

4. Discussion

Application of gentamicin to the stapes footplate resulted in statistically significant hearing loss (8–32 kHz), a reduction in OHCs in the lower basal turn of the cochlea, and a reduction of normal type I HCs in the utricle compared to the same dosage of gentamicin applied to the RWM or the saline controls. These findings suggest that gentamicin may enter the ear more readily through the oval window than through the RWM. If so, the greater hearing loss observed with stapes footplate applications could have resulted from higher drug levels reaching the sensory cells of the cochlea when applied via the vestibule/SV side of the cochlear partition than the RWM/ST. Access of the gentamicin to the inner ear may have been via the annular ligament surrounding the stapes footplate, which presumably has a higher permeability than the RWM. This interpretation is consistent with findings from our previous MRI study (King et al., 2011), which showed higher Gd signal in the vestibule/SV than ST following intratympanic application. The study results were consistent with the Gd directly entering the vestibule in the vicinity of the stapes footplate, a conclusion later confirmed with marker Trimethyphenylammonium (TMPA) using ion-selective microelectrodes sealed into ST and SV following RWM or stapes occlusion with

hydrophobic silicone (Salt et al., 2012). The success of intratympanic gentamicin as a therapy for Mèniére's disease in humans may in part be accounted for by these entry characteristics. If gentamicin enters the inner ear through the annular ligament of the stapes more readily than through the RWM of humans, higher gentamicin concentrations may be achieved in the vestibule compared to scala tympani and this may contribute to the ability to suppress vestibular function while preserving cochlear hair cells and hearing when using optimal gentamicin dosages.

A number of other studies have been consistent with significant drug/marker entry through the OW. MRI studies in humans (Zou et al., 2005) and rats (Zou et al., 2012) showed higher Gd signal intensity in the vestibule than in ST, suggesting that the marker predominately entered in the stapes region rather than the RWM, although in these studies the proportion entering by each route was not quantified. The present study is the first to suggest that, in similarity with Gd, the OW is the primary route for gentamicin to enter the inner ear of guinea pigs following intratympanic administration, rather than entry being dominated by the round window as has been widely accepted up to now.

Even though the RWM has a larger surface area than the annular ligament surrounding the stapes footplate, the anatomical structure of each differs substantially which could account for differing drug permeability between these structures. The RWM in humans, rodents, felines and monkeys is a three-layered structure. An external squamous epithelial layer faces the middle ear cavity, a fibrous subepithelial structure forms the middle layer, and an inner cellular layer contacts the perilymph of ST (Goycoolea & Lundman, 1997; Schachern et al., 1984). The external epithelial layer is a continuous cell layer containing cylindrical cells, ciliated cells with microvilli, and cuboidal cells abundant with mitochondria resting on a basement membrane, allowing it to absorb substances and transport metabolic products (Clark, 2003). Importantly, tight junctions are present near the surface, limiting paracellular movement of solutes (Franke, 1977). The subepithelial layer consists of loose fibrous tissue, capillaries, fibroblasts, fibrocytes, collagen, elastin, vessels and nerve fibers with discontinuous areas of basement membrane that provide space for substances to traverse the membrane (Clark, 2003; Schachern et al., 1984). The endothelial layer in contact with the perilymphatic space consists of squamous cells with long lateral projections, but large intercellular spaces exist (Goycoolea & Lundman, 1997). Factors affecting permeability of the RWM are solute size, configuration, concentration, liposolubility, and electrical charge (Goycoolea et al., 1998). It is reported that tracer substances traverse the RWM either by diffusing through the cytoplasm, as pinocytotic vesicles, or through channels in between cells (Goycoolea & Lundman, 1997). By way of contrast, the stapediovestibular joint (SVJ) in guinea pigs comprises hyaline cartilage on the articulating surfaces of the stapes footplate rim and OW frame, a fluidic articular cavity, and epithelial membranes with tight junctions overlying the structure (middle ear mucosa) as shown in Figure 7. In rats, mice and humans, the stapes is attached to the perimeter of the OW by an annular ligament (Ohashi et al., 2005; Ohashi et al., 2006; Okumura & Iwai-Liao, 1993). The annular ligament consists of a loose thin lattice-like structure of elastic and collagen fibers embedded within a central amorphous substance (Ohashi et al., 2005). The interosseous elastic ligament fibers penetrate the cartilaginous tissues of the frame of the OW and the rim of the stapes footplate and a mantle of fine microfibrils and collagen fibers traverse these elastic fibers (Ohashi et al., 2005; Ohashi et al., 2006). Without tight junctions present, substances would be expected to readily pass through it. Gd entry through the SVJ appears qualitatively similar in guinea pigs and humans using MRI imaging, suggesting the differences in the annular ligament anatomy between these species are not a major factor influencing drug permeability.

The entry of gentamicin into the human inner ear following intratympanic application may be further complicated by the existence of mucosal folds that may cover the round window (false membranes) or tissue plugs, impeding the access of gentamicin to the RWM. It has been estimated that the RWM is obstructed in 33% of humans by secondary (false) membranes, or fibrous plaques (Alzamil & Linthicum, 2000; Plontke, 2011). However, the clinical success of intratympanic gentamicin therapy does not seem consistent with such a high rate of obstruction of the RWM. This discrepancy might be accounted for if a significant proportion of the gentamicin that is applied to the middle ear enters the labyrinth in the region of the stapes.

Although vestibulotoxicity will depend only on the gentamicin concentration in the vestibule, cochleotoxicity could result from drug in either SV or ST. The validity of our primary conclusion, that gentamicin entry occurred preferentially at the stapes, could therefore depend on the kinetic processes by which gentamicin reaches the cochlear hair cells. The possibility that low concentrations of gentamicin in SV could have greater toxicity to the hair cells than higher concentrations in ST therefore has to be considered. There is accumulating evidence that systemically administered gentamicin reaches the hair cells via endolymph, entering the hair cells through the non-specific cation channels in the stereocilia that are associated with mechano-electrical transduction (Dai & Steyger, 2008; Wang & Steyger, 2009, and Wang et al., 2010). Li and Steyger (2011) further showed that systemically-applied fluorescent gentamicin reached the hair cells to a similar degree when ST was irrigated with artificial perilymph to prevent gentamicin accumulation there. The possible routes by which locally-applied gentamicin reaches the cochlear hair cells, and whether an endolymphatic route is significant, has not been studied and remains unknown. In the cochlea, entry from perilymph to endolymph is likely to be limited by the positive endocochlear potential, as gentamicin is cationic in solution. There is presently no evidence suggesting that gentamicin is preferentially taken into endolymph from scala vestibuli perilymph after being applied to the oval window, as would be required if lower concentrations of drug in SV were to explain the greater cochleotoxicity observed here. Furthermore, when the volumes of the vestibule and ST are considered, the vestibule is substantially larger so it would require greater entry at the oval window to generate similar concentrations in SV and ST. If, like other cations (Salt et al., 1991), gentamicin can readily exchange between SV and ST through the spiral ligament or other local pathways, then sustained concentration differences between ST and SV will not be maintained. Therefore, a highly preferential uptake from SV is unlikely as drug applied to either site will have access to both scalae. In view of these considerations, we conclude it is far more likely that the greater toxicity with applications to the stapes is due to a greater entry of gentamicin at stapes than at the round window for a similarly-applied drug dose.

Acknowledgments

This authors wish to thank Mrs Maria Clarke and Miss Prudence Neilson for preparing histology slides; Mrs Ruth Gill for preparing figures; Professor Ian Curthoys for their advice; Sue Pierce and Nicole Joy Christie for providing animal husbandry assistance. Alec Salt was supported by NIH/NIDCD research grant DC 01368 and the project was supported by NHMRC 509206, and the Garnett Passe & Rodney Williams Memorial Fund. This study utilised the Australian Phenomics Network Histopathology and Organ Pathology Service, University of Melbourne.

List of abbreviations

ABR	Auditory brainstem responses
Gd	Gadolinium
GPs	Guinea pigs

HCs	Hair cells
IHCs	Inner hair cells
MRI	Magnetic Resonance Imaging
OHCs	Outer hair cells
OW	Oval window (OW)
RW	Round window
RWM	Round window membrane
ST	Scala tympani
SV	Scala vestibuli
SVJ	Stapediovestibular joint
TMPA	Trimethylphenlyammonium

References

Alzamil KS, Linthicum FH Jr. Extraneous round window membranes and plugs: possible effect on intratympanic therapy. Ann Otol Rhinol Laryngol. 2000; 109:30–32. [PubMed: 10651408]

Clark, G. Cochlear Implants Fundamentals & Applications. Springer Science+Business Media Inc; 2003. p. 71-73.

Dai CF, Steyger PS. A systemic gentamicin pathway across the stria vascularis. Hear Res. 2008; 235(1–2):114–124. [PubMed: 18082985]

Desai SS, Zeh C, Lysakowski A. Comparative morphology of rodent vestibular periphery. I. Saccular and utricular maculae. J Neurophysiol. 2005; 93:251–266. [PubMed: 15240767]

Franke K. Freeze fracture aspects of the junctional complexes in the round window membrane. Arch Otolaryngol Head Neck Surg. 1977; 217:331–337.

Govaerts PJ, Claes J, Van De Heyning Ph, Jorens PHG, Marquet J, De Broe ME. Aminoglycoside-induced ototoxicity. Toxicol Lett. 1990; 52:227–251. [PubMed: 2202080]

Goycoolea MV, Lundman L. Round window membrane. Structure function and permeability: A Review. Microsc Res Tech. 1997; 36:201–211. [PubMed: 9080410]

Goycoolea MV, Muchow D, Schachern PA. Experimental studies on round window membrane structure function and permeability. Laryngoscope. 1998; (Suppl. 44):1–20.

Hirvonen TP, Minor LB, Hullar TE, Carey JP. Effects of intratympanic gentamicin on vestibular afferents and hair cells in the chinchilla. J Neurophysiol. 2005; 93(2):643–655. [PubMed: 15456806]

King EB, Salt AN, Eastwood HT, O'Leary SJ. Direct Entry of Gadolinium into the Vestibule Following Intratympanic Applications in Guinea Pigs and the Influence of Cochlear Implantation. JARO. 2011; 12(6):741–751. [PubMed: 21769689]

Lange G. The intratympanic treatment of Meniere's disease with ototoxic antibiotics. A follow-up study of 55 cases. Laryngol Rhinol Otol. 1977; 56:409–414.

Li H, Steyger PS. Systemic aminoglycosides are trafficked via endolymph into cochlear hair cells. Sci Rep. 2011; 1:159. [PubMed: 22355674]

Lindeman HH. Regional differences in sensitivity of the vestibular sensory epithelia to ototoxic antibiotics. ActaOtolaryngol (Stockh.). 1969; 67:177–189.

Lopez I, Honrubia V, Lee SC, Schoeman G, Beykirch K. Quantification of the process of hair cell loss and recovery in the chinchilla crista ampullaris after gentamicin treatment. Int. J. Dev. Neurosci. 1997; 15:447–461. [PubMed: 9263025]

Lyford-Pike S, Vogelheim C, Chu E, Della Santina CC, Carey JP. Gentamicin is Primarily Localized in Vestibular Type I Hair Cells after Intratympanic Administration. JARO. 2007; 8:497–508. [PubMed: 17899270]

Merchant SN. A Method for Quantitative Assessment of Vestibular Otopathology. Laryngoscope. 1999; 109:1560–1569. [PubMed: 10522922]

Merchant, SN.; Nadol, JB. Schuknecht's Pathology of the Ear. 3rd Edition. People's Medical Publishing House USA; 2010. p. 44-47.

Mikulec AA, Plontke SK, Hartsock JJ, Salt AN. Entry of Substances Into Perilymph Through the Bone of the Otic Capsule After Intratympanic Applications in Guinea Pigs: Implications for Local Drug Delivery in Humans. Otology & Neurotology. 2009; 30:131–138. [PubMed: 19180674]

Nakagawa T, Yamane H, Shibata S, Nakia Y. Gentamicin ototoxicity induced apoptosis of the vestibular hair cells of guinea pigs. Eur Arch Otorhinolaryngol. 1997; 254:9–14. [PubMed: 9115709]

Nakagawa T, Yamane H, Takayama M, Sunami K, Nakai Y. Apoptosis of guinea pig cochlear hair cells following chronic aminoglycoside treatment. Eur Arch Otorhinolaryngol Suppl. 1998; 538:32–35.

Ohashi M, Sawaguchi A, Ide S, Kimitsuki T, Komune S, Suganuma T. Histochemical Characterization of the Rat Ossicular Joint Cartilage with a Special Reference to Stapediovestibular Joint. Acta Histochem Cytochem. 2005; 38(6):387–392.

Ohashi M, Idc S, Kimitsuki T, Komune S, Suganuma T. Three-dimensional regular arrangement of the annular ligament of the rat stapediovestibular joint. Hear Res. 2006; 213:11–16. [PubMed: 16476532]

Okumura A, Iwai-Liao Y. Developmental anatomy of the mouse stapediovestibular and temporomandibular joints. Okajimas Folia Anat Jpn. 1993; 69:385–400. [PubMed: 8469528]

Plontke SKR, Wood AWW, Salt AN. Analysis of Gentamicin Kinetics in Fluids of the Inner Ear with Round Window Administration. Otol Neurotol. 2002; 23:67–974. [PubMed: 11773850]

Plontke SKR, Mynatt R, Gill RM, Salt AN. Concentration gradient along scala tympani following the local application of gentamicin to the round window membrane. Laryngoscope. 2007; 117:1191–1198. [PubMed: 17603318]

Plontke SK. Evaluation of the round window niche before local drug delivery to the inner ear using a new mini-otoscop. Otol Neurotol. 2011; 32:183–185. [PubMed: 21192347]

Quaranta A, Aloisi A, De Benedittis G. Scaringi A. Intratympanic therapy for Ménière's disease. High-concentration gentamicin with round-window protection. Ann N Y Acad Sci. 1999; 884:410–424. [PubMed: 10842610]

Saijo S, Kimura RS. Distribution of HRP in the inner ear after injection into the middle ear cavity. Acta Otolaryngol. 1984; 97:593–610. [PubMed: 6464711]

Salt AN, Ohyama K, Thalmann R. Radial communication between the perilymphatic scalae of the cochlea. II: Estimation by bolus injection of tracer into the sealed cochlea. Hear Res. 1991; 56(1–2):37–43. [PubMed: 1769923]

Salt AN, Ma Y. Quantification of solute entry into cochlear perilymph through the round window membrane. Hear Res. 2001; 154:88–97. [PubMed: 11423219]

Salt AN, Kellner C, Hale S. Contamination of perilymph sampled from the basal cochlear turn with cerebrospinal fluid. Hear Res. 2003; 182:24–33. [PubMed: 12948598]

Salt AN, Gill RM, Plontke SK. Dependence of Hearing Changes on the Dose of Intratympanically Applied Gentamicin: A Meta-Analysis Using Mathematical Simulations of Clinical Drug Delivery Protocols. Laryngoscope. 2008; 118(10):1793–800. [PubMed: 18806480]

Salt AN, King EB, Hartsock JJ, Gill RM, O'Leary SJ. Marker Entry into Vestibular Perilymph via the Stapes Following Applications to the Round Window Niche of Guinea Pigs. Hear Res. 2012; 283(1–2):14–23. [PubMed: 22178981]

Schachern PA, Paparella MM, Duvall AJ, Choo YB. The human round window membrane. An electron microscopic study. Arch Otolaryngol. 1984; 110:15–21. [PubMed: 6689900]

Shepherd RK, Colreavy MP. Surface microstructure of the perilymphatic space: implications for cochlear implants and cell- or drug-based therapies. Arch Otolaryngol Head Neck Surg. 2004; 130(5):518–523. [PubMed: 15148170]

Silverstein H, Arruda J, Rosenberg S, Deems D, Hester O. Direct round window membrane application of gentamicin in the treatment of Meniere's disease. Otolaryngol Head Neck Surg. 1999; 120:649–655. [PubMed: 10229588]

Tanaka K, Motomura S. Permeability of the labyrinthine windows in guinea pigs. Arch Otorhinolaryngol. 1981; 233:67–73. [PubMed: 6976164]

Tanyeri H, Lopez I, Honrubia V. Histological evidence for hair cell regeneration after ototoxic cell destruction with local application of gentamicin in the chinchilla crista ampullaris. Hearing Research. 1995; 89:194–202. [PubMed: 8600126]

Tsuji K, Velázquez-Villaseñor L, Rauch SD, Glynn RJ, Wall C 3rd. Merchant SN. Temporal bone studies of the human peripheral vestibular system. Aminoglycoside ototoxicity, Ann Otol Rhinol Laryngol Suppl. 2000; 181:20–25.

Wang Q, Steyger PS. Trafficking of systemic fluorescent gentamicin into the cochlea and hair cells. J Assoc Res Otolaryngol. 2009; 10(2):205–219. [PubMed: 19255807]

Wang Q, Kachelmeier A, Steyger PS. Competitive antagonism of fluorescent gentamicin uptake in the cochlea. Hear Res. 2010; 268(1–2):250–259. [PubMed: 20561573]

Zou J, Pyykkö I, Bjelke B, Dastidar P, Toppila E. Communication between the Perilymphatic Scalae and Spiral Ligament Visualized by in vivo MRI. Audiol Neurotol. 2005; 10:145–152.

Zou J, Poe D, Ramadan UA, Pyykkö I. Oval Window Transport of Gd-DOTA From Rat Middle Ear to Vestibulum and ScalaVestibuli Visualized by In Vivo Magnetic Resonance Imaging. Annals of Otology, Rhinology & Laryngology. 2012; 121(2):119–128.

Highlights

1. Gentamicin entered the inner ear when applied to the stapes footplate
2. Greater hearing loss occurred when gentamicin was applied to the stapes footplate
3. There were fewer outer hair cells in the basal turn of the cochlea when gentamicin was applied to the stapes
4. There were fewer type I hair cells in the utricle when gentamicin was applied to stapes

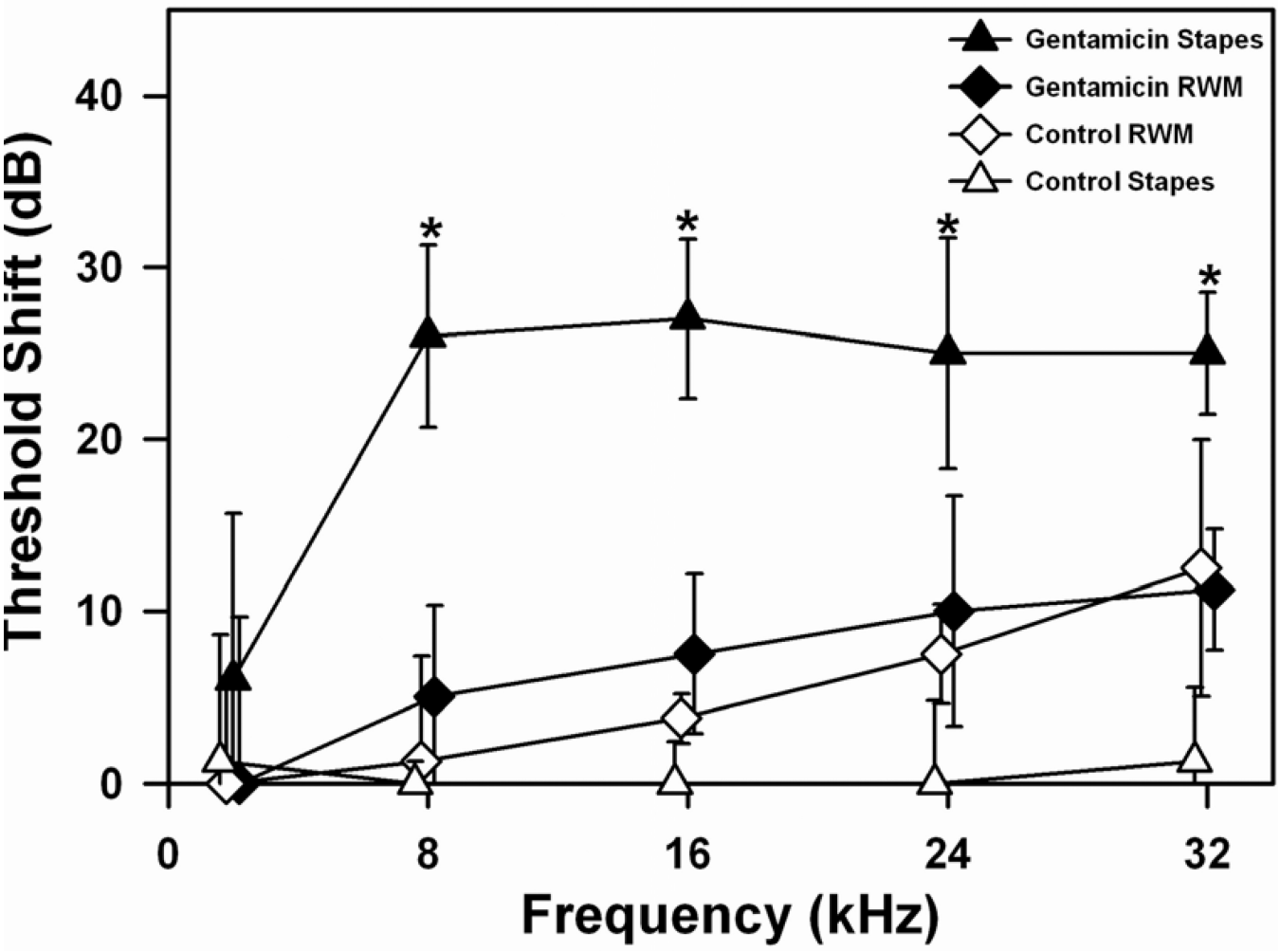

Figure 1.

ABR threshold shifts at 5 stimulus frequencies measured 1 week following gentamicin or saline administration on the stapes footplate or round window membrane (RWM). Bars indicate SEM. Statistically significant threshold elevations were observed following gentamicin administration to the stapes footplate at 8, 16, 24 and 32kHz, compared to RWM and to both saline control cohorts. Threshold shifts at 8, 16 and 24 kHz following gentamicin administration to the RWM were higher than their saline controls, but not significantly so. The larger hearing loss when gentamicin was applied to the stapes footplate suggests more gentamicin entered the labyrinth in that condition.

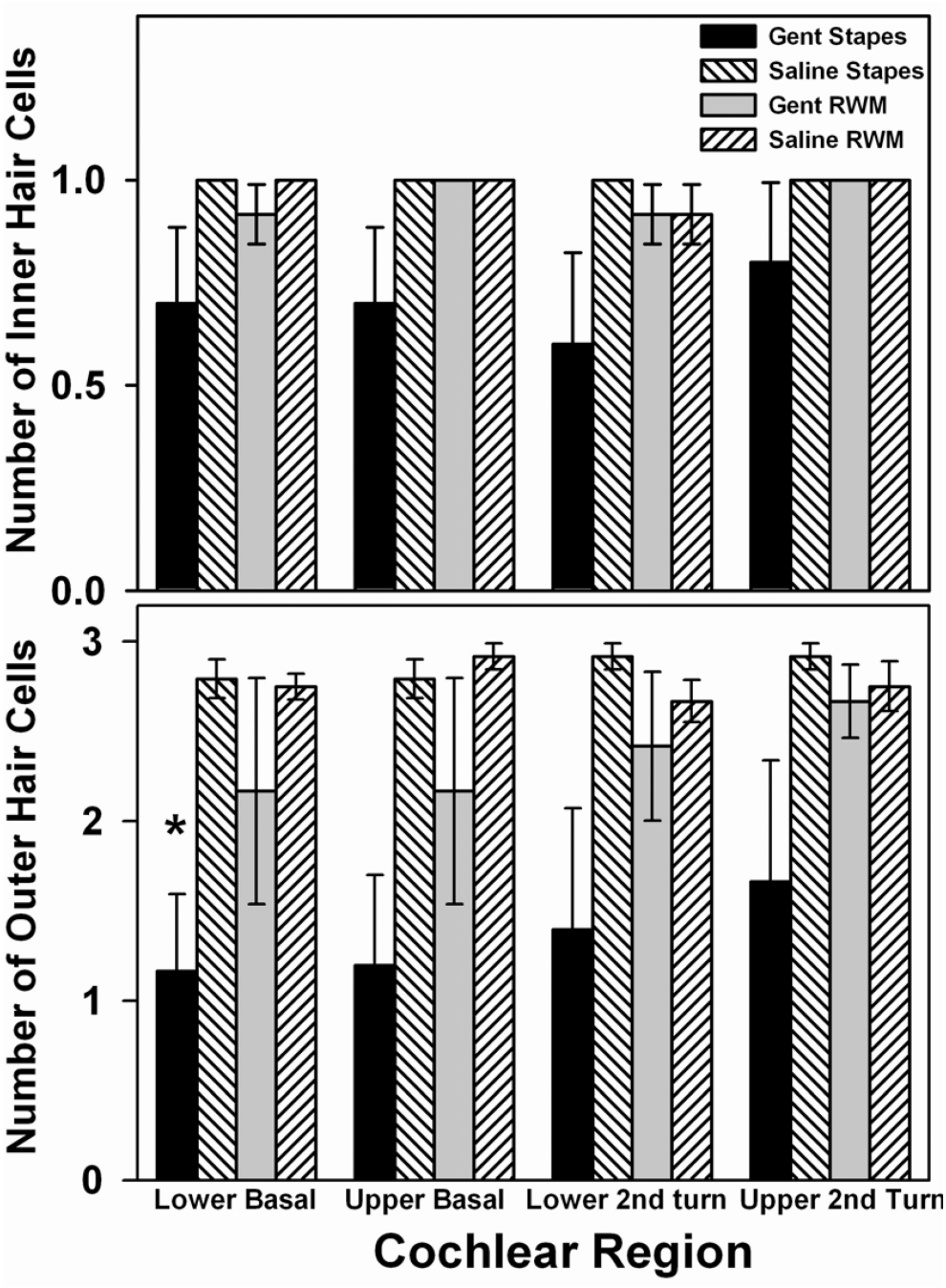

Figure 2.

Effects of gentamicin application protocols on cochlear hair cells. Outer and inner hair cell counts in the lower and upper regions of the basal and second turns in the cochlea averaged over 3 consecutive sections, each spaced 50 μm apart. Numbers of surviving hair cells when gentamicin was applied to the stapes or round window membrane are compared to saline controls. The reduction of outer hair cells in the lower basal turn following gentamicin administration on the stapes footplate was statistically significant compared to saline applied on the stapes. Error bars indicate SEM.

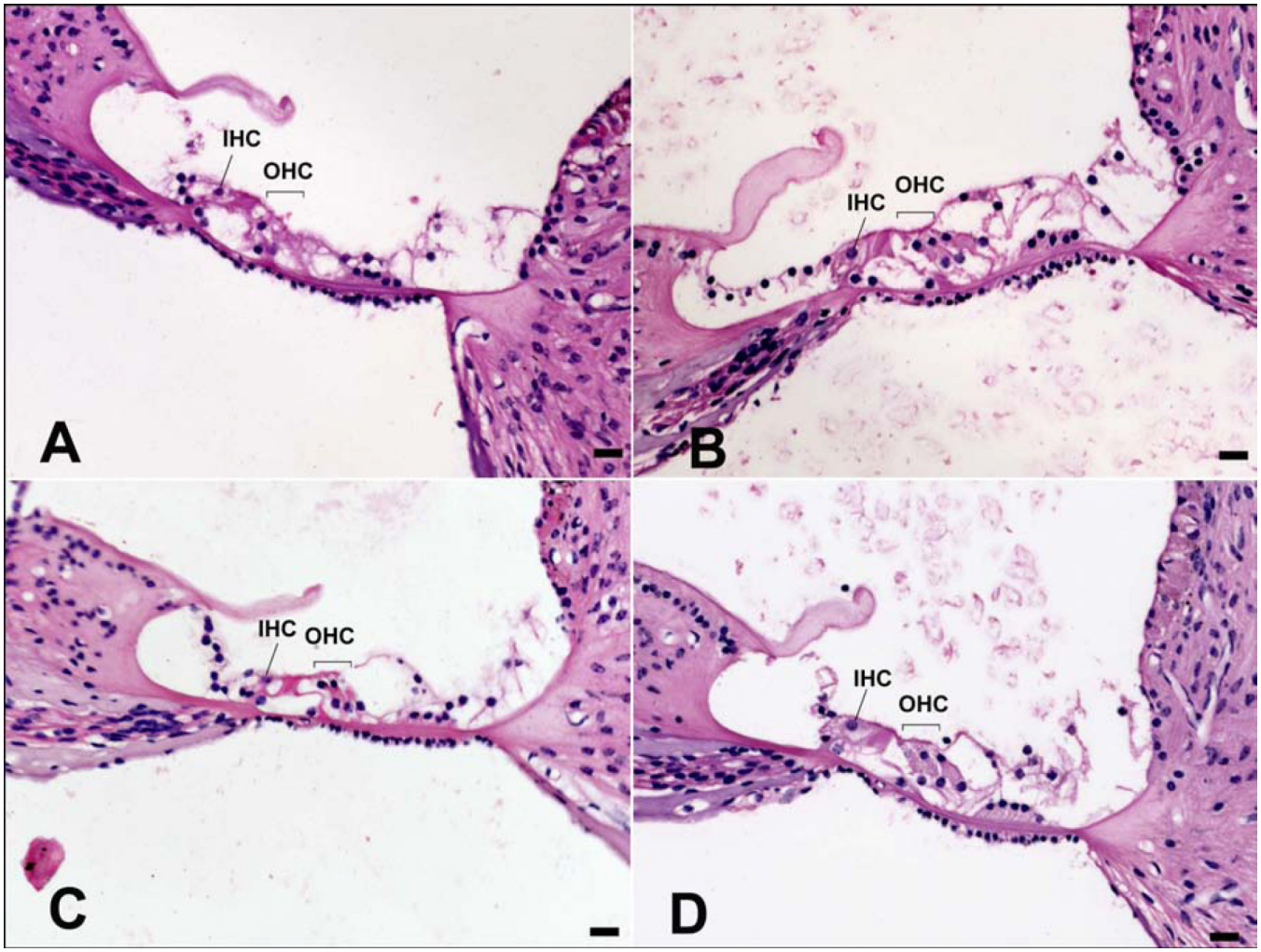

Figure 3.
Examples of average hair cell morphology in the lower basal turn of the cochlea from each treatment group shown in Haematoxylin and Eosin stained sections. IHC: Inner hair cell, OHC: Outer hair cells. 20x magnification, scale bars = 20 μm. **A**) Gentamicin applied to the stapes footplate. **B**) Gentamicin applied to the round window membrane (RWM). **C**) Saline applied to the stapes footplate. **D**) Saline applied to the RWM.

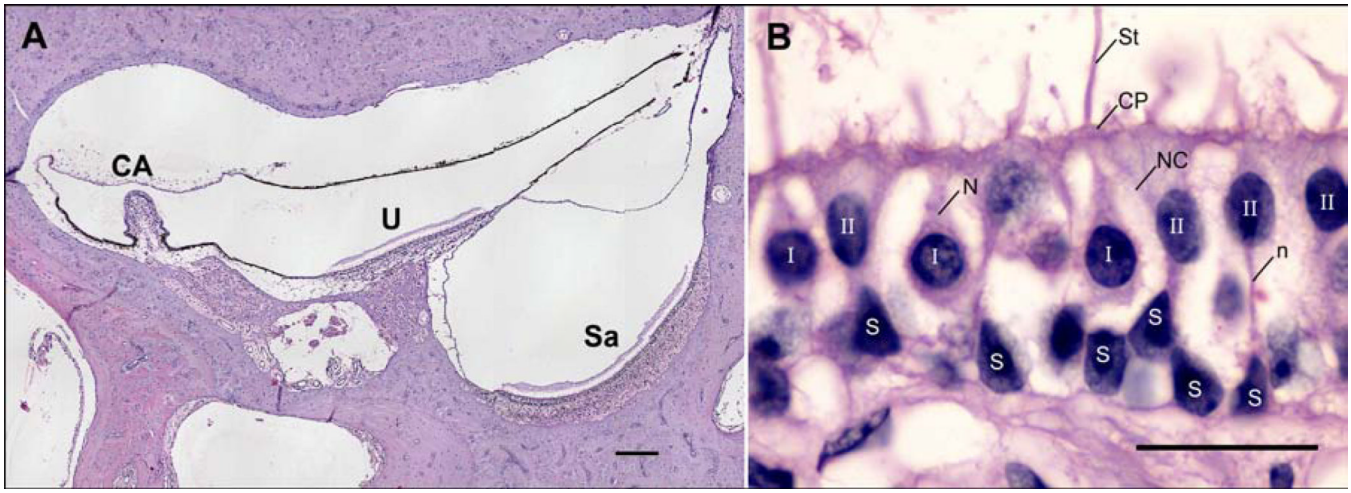

Figure 4.

Regions of interest and characterisation of the cell types counted in the vestibule in Haematoxylin and Eosin stained sections. **A**) Vestibular regions analysed. CA: crista ampullaris in posterior semicircular canal ampulla, U: utricular macula, Sa: macula of saccule. 10x magnification, scale bar = 200 μm. **B**) Cell types. I: Normal type I hair cell characterized by a spherical nucleus with substantially heterogeneous chromatin, a thick nerve branch (N) surrounded by flask-shaped nerve calyx (NC) with a narrowing toward the cuticular plate (CP), and stereocilia (St). II: Type II hair cell characterized by cylindrical shape, oval nucleus with substantially homogenous chromatin, nerve branch (n) without a nerve calyx surrounding the cell body, and spatial location closer to the cuticular plate than supporting cells. S: Supporting cell characterized by a nucleus with chromatin material distributed in clumps, spatial location adjacent to the basal lamina, and a lack of stereocilia or cuticular plate. 100x magnification, scale bar = 20 μm.

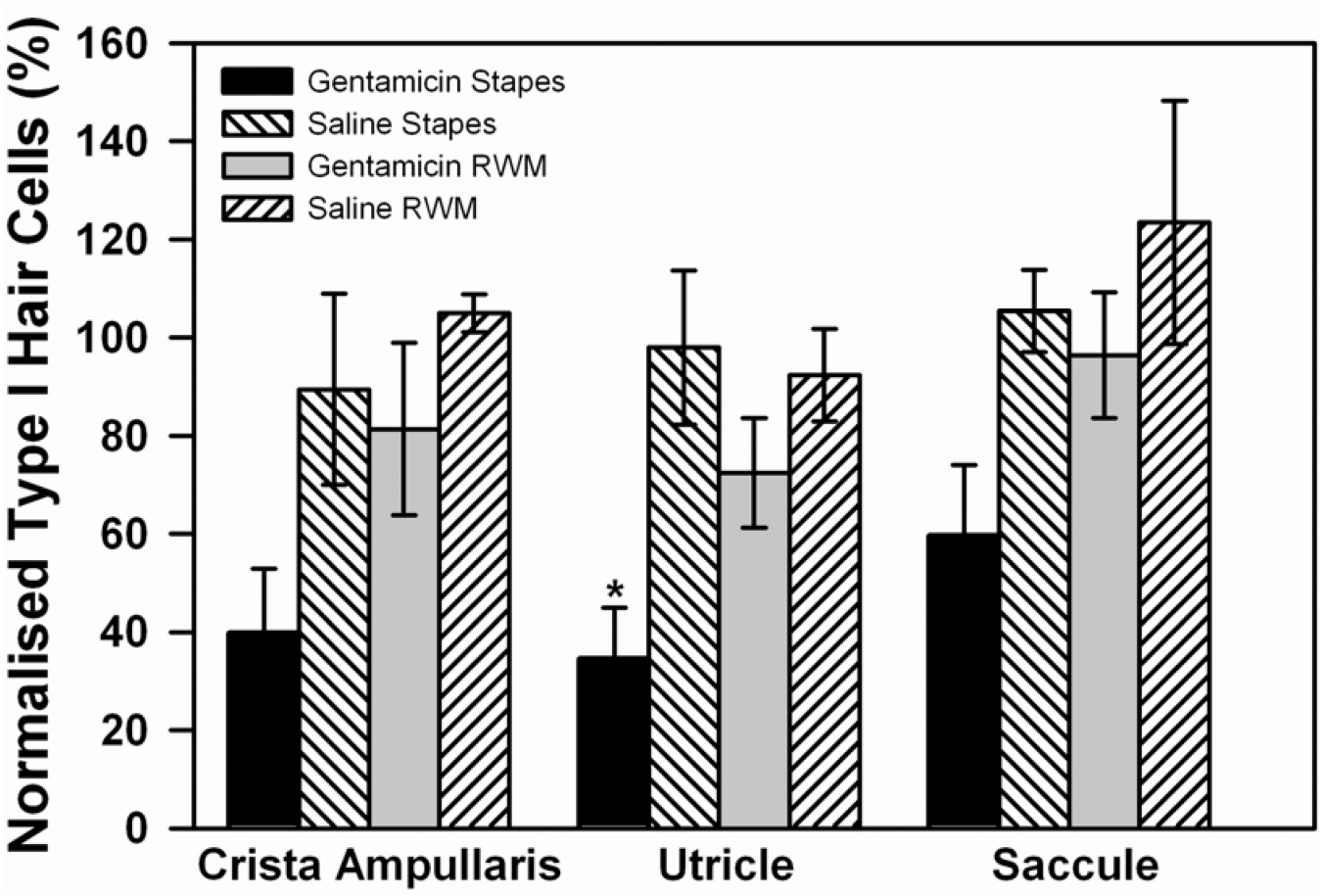

Figure 5.
Type I hair cell counts in the mid-section of crista ampullaris of the posterior semi-circular canal, the utricular macula, and the saccular macula in the vestibule. Cell counts were compared for gentamicin or saline applications to the stapes or round window membrane (RWM). In all groups, counts of morphologically normal type I hair cells were normalized with respect to those of the untreated, contralateral ear. Error bars indicate SEM.

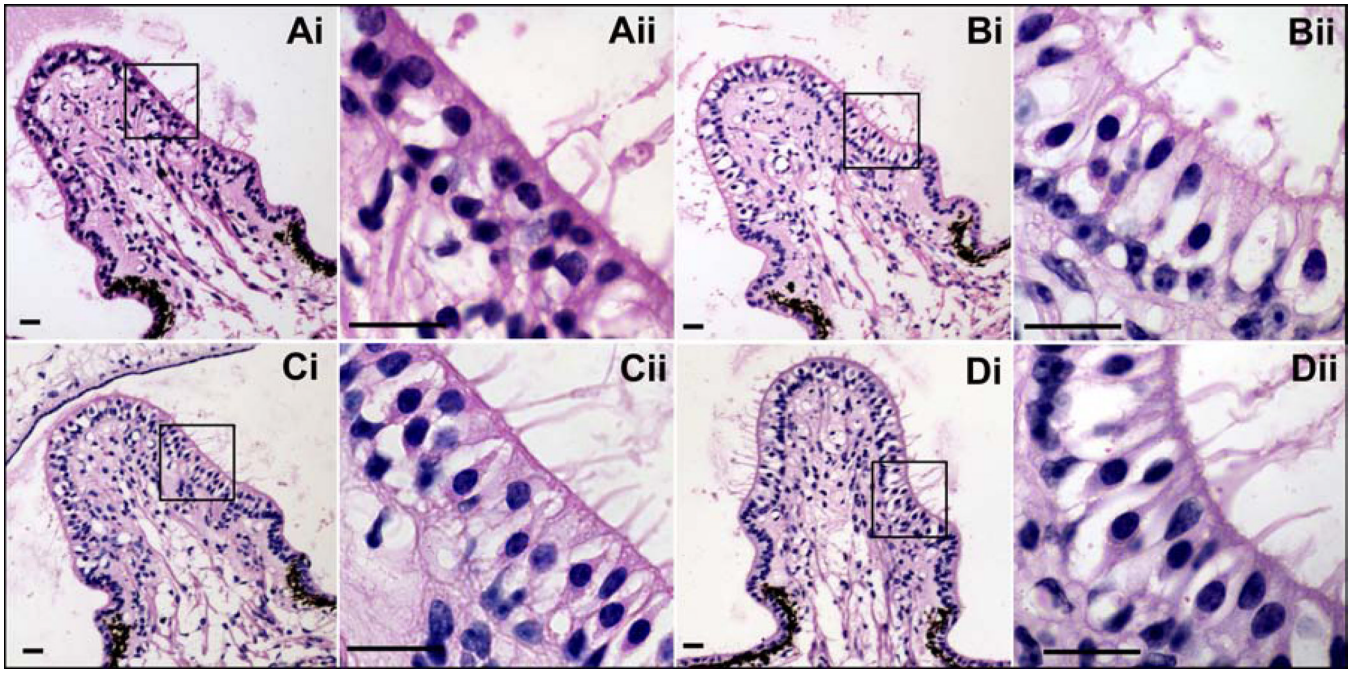

Figure 6.

Gentamicin-induced morphological changes in crista ampullaris of the posterior lateral semicircular canal in Haematoxylin and Eosin stained sections. Low power magnification: 20x objective, scale bar = 20 mm. Higher power magnification images: 100x objective, scale bar = 20 mm. **Ai**) Gentamicin administration on the stapes footplate. Extensive damage was caused to type I and type II hair cells characterized by calyceal distortion and lucency, reduced hair cells and stereociliary bundles, and a narrowing of the cellular layer between the cuticular plate and basal lamina. **Bi**) Gentamicin administration on the round window membrane. The majority of cells exhibited normal morphological appearance although some damage was caused to type I hair cells. **Ci**) Saline administration on the stapes footplate. **Di**) Saline administration on the round window membrane. **Aii**-**Dii**) are higher magnifications of the outlined areas shown in Ai-Di respectively.

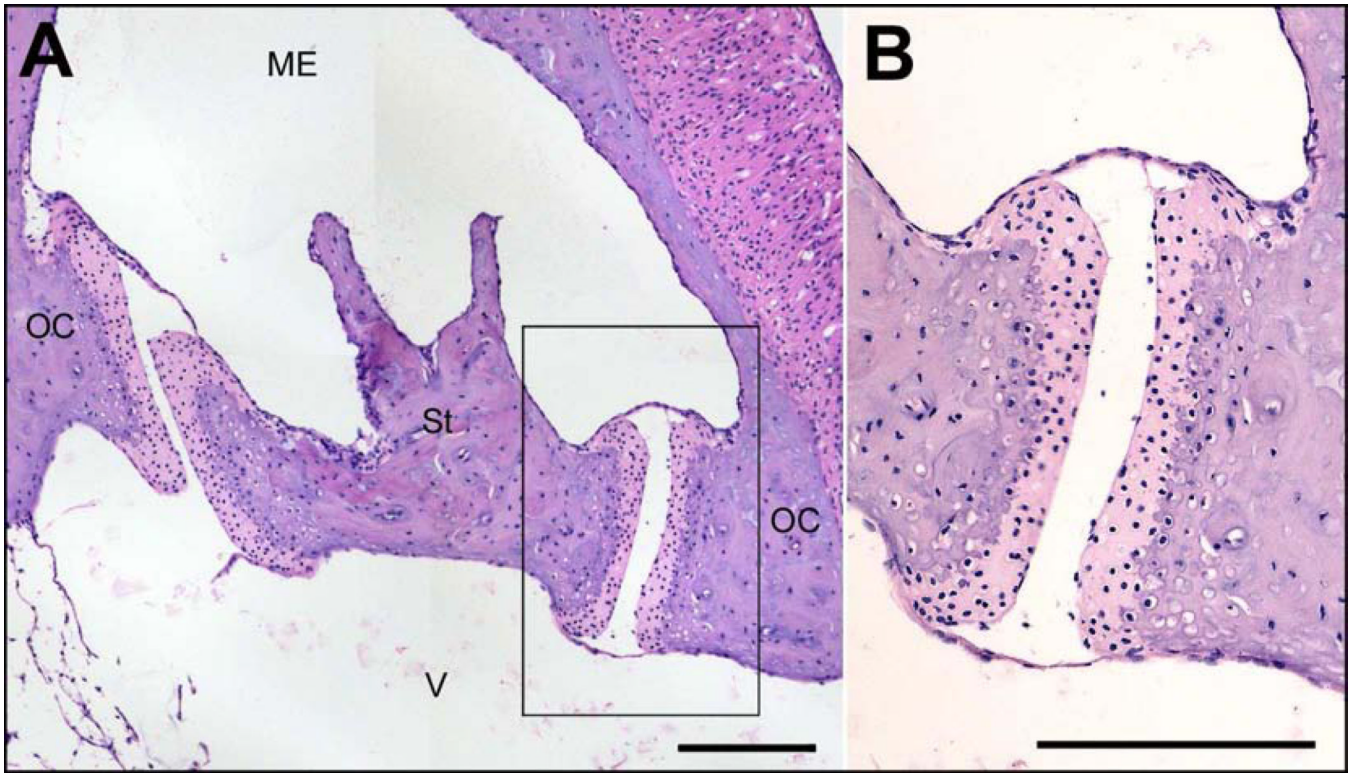

Figure 7.

A) Cross-section of the stapes and stapediovestibular joint (SVJ) of a guinea pig. St: stapes, OC: oval window frame in the otic capsule, ME: middle ear space, V: vestibule. 10x magnification, scale bar = 200μm. **B**) Magnification of boxed area. The SVJ comprises hyaline cartilage (light pink) on the articulating surfaces of the stapes footplate rim and oval window frame, a fluidic articular cavity, and epithelial membranes with tight junctions overlying the structure (middle ear mucosa). 20x magnification, scale bar = 200μm.